Journal of Nuclear Materials 386–388 (2009) 666–669

Contents lists available at ScienceDirect

Journal of Nuclear Materials

journal homepage: www.elsevier.com/locate/jnucmat

Influence of local crystallographic orientation on short crack propagation in high cycle fatigue of 316LN steel

Emilie FERRIE [a,*], Maxime Sauzay [b]

[a] SIMAP – GPM2, UMR 5266, Grenoble-INP, 101 Rue de la physique, 38402 Saint Martin d'Hères, France
[b] DMN-SRMA-LA2M, CEA Saclay, 91191, Gif-sur-Yvette, France

A B S T R A C T

In this study, three dimensional finite element calculations taking into account *cubic elasticity* and *crystalline plasticity* are performed in order to quantify the influence of the crystallographic orientation on the development of the plasticity at the crack tip of *microstructurally short cracks* in *316L stainless steel*. The case of a *transgranular stage I crack* that 'propagates' towards a grain oriented for *multiple slip* is considered. The values of the *crack tip opening/sliding displacements* are calculated for the crack located at different distances of the 'multiple slip' grain. Two multiple slip orientations are considered for this adjacent grain: a $\langle 1\,1\,1\rangle$ orientation and a $\langle 1\,\bar{1}\,0\rangle$ orientation. Calculations show that the opening/sliding displacement at the crack tip is higher (up to a factor 1.7) if the crack propagates towards a $\langle 1\,\bar{1}\,0\rangle$ grain than towards a $\langle 1\,1\,1\rangle$ grain. This could imply that propagation towards a $\langle 1\,1\,1\rangle$ grain is more difficult than towards a $\langle 1\,\bar{1}\,0\rangle$ grain.

1. Introduction

Austenitic stainless steel 316L(N) has been selected for vessel and in-vessel components of ITER. Its low cycle fatigue properties have been extensively studied [1–3]. This paper extends the investigations to the *high cycle* fatigue regime, where a large scatter in results is observed, making life assessment of nuclear power plant components difficult.

In the high cycle fatigue regime, microstructurally short cracks (*i.e.* cracks with a size comparable to the grain size) generally initiate during the first thousand cycles. The major part of the total fatigue life would hence be dedicated to the *propagation* of short cracks [4]. During their propagation, these short cracks strongly interact with grains, which would suggest that the local variability of the crystallographic orientation may contribute to the scatter observed experimentally between samples [5]. In this paper, the cause of this large scatter is examined through finite element simulations of short fatigue crack propagation from one grain into the neighbouring grain.

More precisely, the propagation of a short crack from one grain to another is governed by its ability to develop *cyclic plasticity at the crack tip* depending on the local crystallography. To better understand short crack *propagation*, a first step is hence to simulate and *quantify* the development of *cyclic plasticity at the tip* of a crack propagating *along a slip plane* in the case of different crystallographic configurations.

In this aim, three dimensional (3D) elastic–plastic finite element (FE) calculations taking into account elastic–plastic *crystalline anisotropy* are performed. A simple post processing routine is used to calculate the displacements at the crack tip. The results obtained for two *multiple slip* crystallographic configurations will be compared.

2. Finite element mesh of the crack and the grains

From an experimental point of view, fatigue crack propagation in 316L stainless steel is a complicated process that involves intergranular, transgranular propagation as well as interaction with twins. For the sake of simplicity, in the modelling, we will consider the case of a *stage I fatigue* crack initiated in a grain called *G1* located at the sample surface (see Fig. 1(b)). This grain containing crack is oriented for *easy slip* (Schmid factor of 0.5) and slip occurs along the $\langle 1\,1\,1\rangle$ crystallographic plane in the [1–10] direction (see Fig. 1(a)). The crack is located on this slip plane and the direction of *G*., and hence, the crack front is along the *z*-axis as represented in Fig. 1(b)). As we are interested in the influence of local crystallographic orientation on crack propagation, we will also consider the grain adjacent to *G1*, which is called *G2* (see Fig. 1(b)). Grains have the shape of a hexagon (or part of it) inscribed in a circle of 50 μm diameter that corresponds to the average grain size of 316L stainless steel [6–8].

The grain containing crack, *G1*, and its neighbouring grain, *G2*, are embedded in a matrix that represents the polycrystalline medium (see Fig. 1). In order to capture large stress and strain gradients at the crack tip, a radius of curvature of 100 nm,as well as a very

* Corresponding author.
E-mail address: Ferrie@gpm2.inpg.fr (E. FERRIE).

0022-3115/$ - see front matter © 2008 Elsevier B.V. All rights reserved.
doi:10.1016/j.jnucmat.2008.12.261

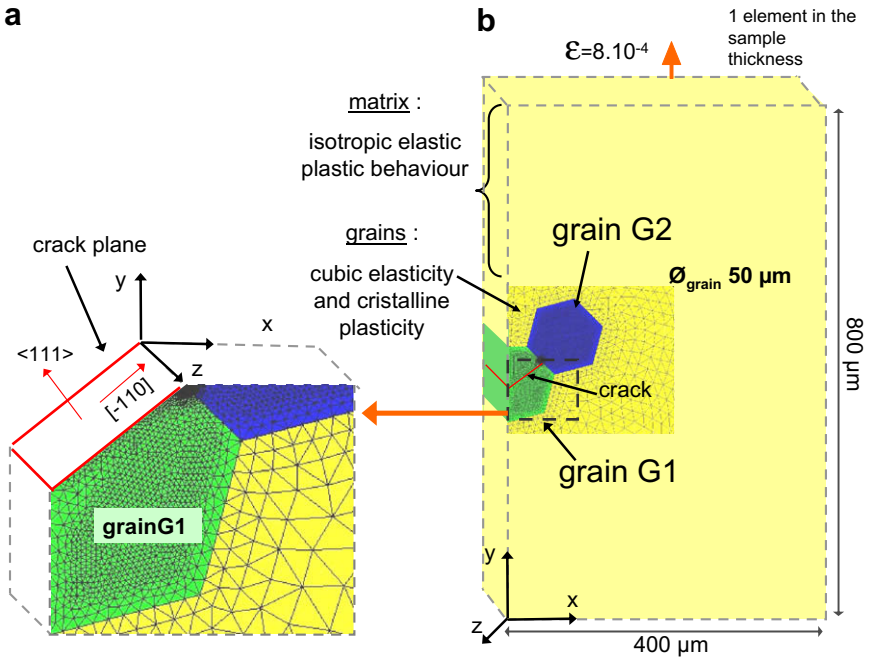

Fig. 1. Finite element mesh representing grain *G1* containing the stage I crack, the adjacent grain *G2* and the surrounding polycrystalline matrix. The displacement is applied on the upper surface along the *y*-axis.

fine radial mesh with cubic elements, are used to model the crack tip. To mimic crack propagation towards *G2*, five different meshes with a crack size varying from 21.5 μm to 28 μm have been generated.

The previously described 2D mesh is extruded along the *z*-axis (see Fig. 1) in order to create a 3D mesh of 0.5 μm thick (plane stress problem) and containing one element in the thickness. The mesh geometry is 'pseudo 3D' but the FE calculations are 3D as the *12 slip systems* of the FCC crystallographic structure are taken into account. Particular grains that exhibit *multiple slip activity* can hence be modelled.

The finite element mesh as well as the calculations crack tip opening/sliding displacements described in hereafter are performed using the 3D elastic–visco–plastic finite element code developed at the CEA called *Cast3m.*

3. Mechanical models for the grains and the surrounding matrix

3.1. Mechanical model for the grains: cubic elasticity and crystalline plasticity

Elastic behaviour: considering the strong *elastic anisotropy* of 316L stainless steel ($2C_{44}/(C_{11}-C_{12}) \sim 3.36$), cubic elasticity of the grains is taken into account in the FE calculations. The values of the elastic constants used are $C_{11} = 197.5$, $C_{12} = 125$ and $C_{44} = 122$ GPa.

Plastic behaviour (hardening law): The hardening law governs the evolution of the shear stress on each slip system of the grains. In order to model as well as possible the cyclic behaviour of the *grains,* the choice of the hardening law is based on experimental observations performed by Laird et al. [9] on stainless *steel single crystals*. These authors observed that the increase of the *stabilized* resolved shear stress for increasing values of applied plastic strain is mainly due to the contribution of the back stress (long range dislocations interactions) as the friction stress decreases slightly (short range interactions). In our model, the *friction stress* is assumed to remain constant (no isotropic hardening); and the evolution of *the back stress* τ_x^s is governed by a *non linear kinematics hardening law (see Eq. (1).)*

$$d\tau_x^s = \frac{2}{3}A \cdot d\gamma^s - B \cdot \tau_x^s \cdot |d\gamma^s| \quad (1)$$

where $d\gamma^s$ is the increment of plastic slip on each system.

The crystalline constitutive laws have been introduced in *Cast3m, via* UMAT[1] procedures that have been built from sub-routines initially implemented by Heraud [10].

To determine the values of the coefficients A and B, inverse identification is generally used. However, this method is not so appropriate to account for the *local* behaviour of the*grain*. Therefore, in this study, identification using cyclic strain stress curves obtained on *stainless steel single crystal* by Gorlier et al. [11] is preformed instead. Further details on the identification can be find in [12].

3.2. Mechanical model for the material surrounding the grains

The elastic behaviour of the matrix surrounding the grains is assumed to be *isotropic* with a Young modulus of 185 GPa. Its stabilized cyclic plastic behaviour is described using a non-linear kinematic hardening law identified using cyclic strain stress curves obtained on 316L polycrystals by different authors [6–8].

4. Calculations of the opening and sliding displacements at the crack tip

4.1. Definitions of CTOD and CTSD

The crack tip opening displacement (CTOD) and the crack tip sliding displacement (CTSD), defined in Fig. 2, are calculated in the local axes ($\boldsymbol{m}$, $\boldsymbol{n}$) of the crack tip where $\boldsymbol{m}$ is the Burgers vector

[1] UMAT routines are subroutines developed by the user in order to introduce in a finite element code (such as *Cast3m) a* specific user-defined mechanical laws and material properties.

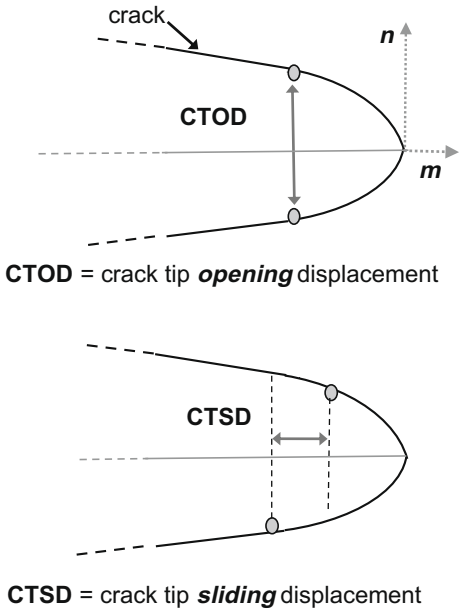

Fig. 2. Schematic representation of the crack tip opening displacement and crack tip sliding displacement. The vector ***m*** is the slip direction and ***n*** is the normal to the slip plane.

(slip direction) and ***n*** the normal to the slip plane. The CTOD can be defined as the displacement in the ***n*** direction of the lower part of the crack with respect to the upper part. Similarly, the CTSD is the displacement along the sliding direction ***m***.

4.2. Calculations of CTSD and CTOD for different crystallographic orientations for grain G2

The upper sample surface is subjected to a displacement along the *y*-axis which results in a macroscopic strain of 8.10^{-4} (Fig. 1). Only a monotonic loading is applied, but as the hardening law used account for the *stabilized* strain stress behaviour, such a monotonic analysis would give a good approximation of cyclic behaviour at the crack tip.

To quantify the influence of the crystallographic orientation on the development of the plasticity at the crack tip in grain *G1*, the CTSD and CTOD are calculated considering two different *multiple slip* crystallographic orientations for the grain *G2* and keeping the orientation of *G1* constant ($F = 0.5$: easy slip):

- *G1*/⟨1 1̄ 0⟩ configuration: *G2* is a ⟨1 1̄ 0⟩ grain with *4 slip systems* and $F = 0.408$ (see Fig. 3).
- *G1*/⟨1 1 1⟩ configuration: *G2* is a ⟨1 1 1⟩ with *6 slip systems* and $F = 0.27$ (see Fig. 4).

For each *G1/G2* configuration, in order to mimic crack propagation towards the grain boundary, the calculations are performed considering the crack tip at different distances, *d*, from the grain boundary (*d* is defined in Figs. 3 and 4(a)). The evolution of CTSD and CTOD for different values of *d* are represented in Fig. 3(b) for *G1*/⟨1 1̄ 0⟩ configuration and Fig. 4(b) for *G1*/⟨1 1 1⟩.

For *G1*/⟨1 1̄ 0⟩ configuration, the values of the CTOD and CTSD increase as the crack gets closer to the grain boundary. For the *G1*/⟨1 1 1⟩ configuration, the CTOD and CTSD values increase between 7.5 μm and 5 μm with the same trend as for *G1*/⟨1 1̄ 0⟩ configuration. However, for $d > 5$ μm, CTOD and CTSD remain nearly constant. And even a slight decrease is observed for $d < 1$ μm which would suggest that the grain ⟨1 1 1⟩ prevents the development of the crack tip plasticity.

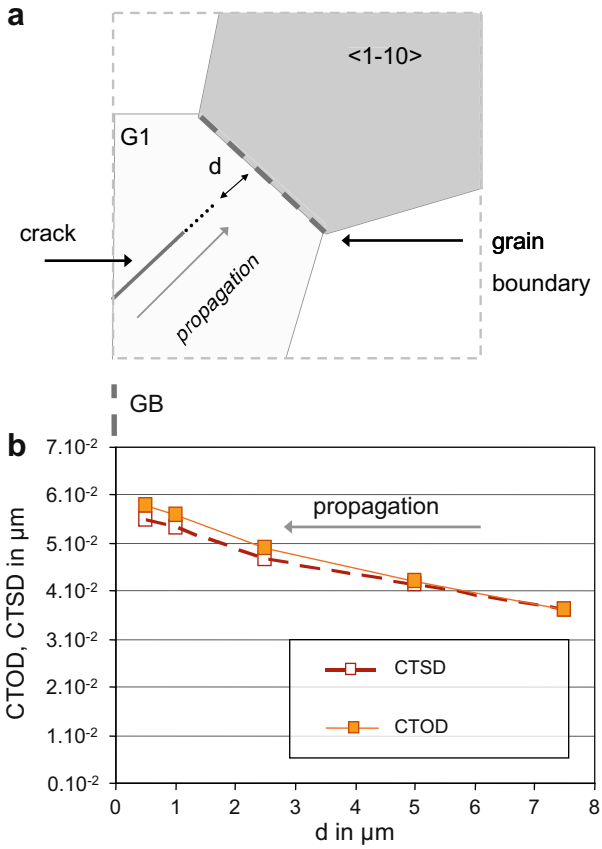

Fig. 3. (a): Schematic representation of the crack located at a distance *d* to the grain boundary between *G1* and the ⟨1 1̄ 0⟩ grain (4 slip systems with a Schmid factor of 0.408). (b) Evolution of the CTOD and CTSD with *d*, defined as the distance between the crack tip and the grain boundary along the [1̄ 1 0] direction; decreasing values of *d* correspond to the propagation towards grain ⟨1 1̄ 0⟩.

At 0.5 μm from the crack tip, the CTSD/CTOD values in the *G1*/⟨1 1̄ 0⟩ are respectively 1.7 times and 1.55 times higher than in the *G1*/⟨1 1 1⟩ configuration. Post processing analysis shows that the total plastic slip at the crack tip is of 13% for the *G1*/⟨1 1 1⟩, and reach the value of 18% for *G1*/⟨1 1̄ 0⟩, which is coherent with the CTOD and CTSD values obtained.

Mesh sensitivity has been investigated and the values of CTSD and CTOD calculated with a mesh 4 times finer are represented in Fig. 4(b). Other calculations have been performed and show that the influence of the mesh size is around 5%, which is much smaller than the difference of CTOD and CTSD observed between the two different crystallographic configurations studied.

4.3. Crack growth and crystallographic orientation

The correlation between fatigue crack growth rate and CTOD for microstructurally short crack have been observed experimentally in 316L by Blochwitz et al. [13]. The difference between the value of CSTD and CTOD computed for two different crystallographic configurations can be hence interpreted in terms of propagation rate: crack propagation would be easier towards a ⟨1 1 1⟩ grain than a ⟨1̄ 1 0⟩ grain.

The influence of the orientation of the neighbouring grain on CTSD/CTOD values has been also shown by Bennett et al. using a *2D* planar slip model where only *2 systems* among the 12 slip systems of the FCC are considered [14]. Simonovski et al. performed also 2D calculations but only *single slip grains* have been considered (no multiple slip grains) [15]. 3D calculations, but only for a mode I

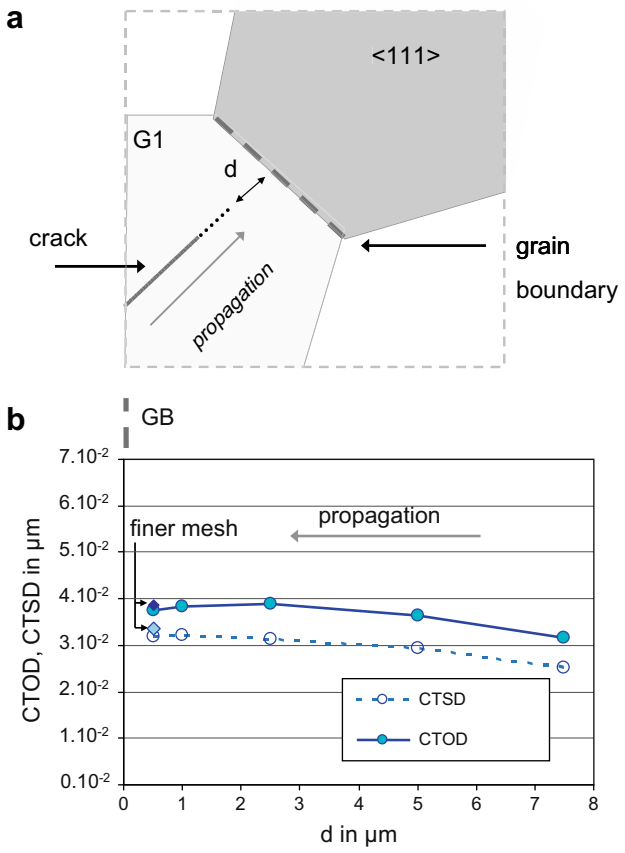

Fig. 4. (a): Schematic representation of the crack located at a distance d to the grain boundary between *G1* and a ⟨1 1 1⟩ grain (6 slip systems with a Schmid factor of 0.27). (b)) Evolution of the CTOD and CTSD with *d*, defined as the distance between the crack tip and the grain boundary along the [1–10] direction; decreasing values of *d* correspond to the propagation towards grain ⟨1 1 1⟩.

crack in a single crystal (no grain neighbouring grain effect) have also been performed by Johnston et al. [16]. Therefore, our approach is rather original as it is 3D and focuses on the effect of a 'multiple slip neighbouring grain' on the crystallographic propagation (*i.e* along a slip plane) of a short crack.

5. Conclusions

In this study, a *stage I* crystallographic crack and its adjacent grain embedded in a polycrystalline matrix have been modelled using a 3D elastic–plastic finite element code taking into account cubic elasticity and crystalline plasticity. The adjacent grain is considered to be a *multiple slip* grain (⟨1 1 1⟩ or ⟨1 $\bar{1}$ 0⟩) and its influence on values of the opening/sliding displacements (CTOD and CTSD) at the crack tip of the stage I crack has been investigated. Values of displacements have been calculated for the crack located at different distances from the grain boundary in order to mimic crack propagation. Care has been taken to chose and identify a hardening law using experimental data obtained on *single crystals*.

Calculations show that the values of the CTOD/CTSD in the grain *G1* depend on the crystallographic orientations of the neighbouring grain. For the *G1*/⟨1 $\bar{1}$ 0⟩ configuration, the CTOD/CTSD values increase*continuously* when the crack approaches the grain ⟨*1* $\bar{1}$ *0*⟩. For the *G1*/⟨*1 1 1*⟩ configuration, the CTOD/CTSD values are lower (up to a factor 1.7) and exhibit only a slight increase and even decrease as the crack gets closer to the grain boundary. It would imply that ⟨1 1 1⟩ orientated grain do not favour crack propagation.

References

[1] F. Tavassoli, Assessment of Austenitic Stainless Steels – Proceeding of Int. Symposium on Fusion Nuclear Technology-3, Fus. Eng. Desig, vol. C, 1995.
[2] J.-A. Le Duff, P. Ould, J.-L. Bernard, Int. J. Pressure Vessels Piping 65 (3) (1996) 241.
[3] W.-Y. Maeng, M.-H. Ki, J. Nucl. Mater. 282 (1) (2000) 32.
[4] K.J. Miller, Fatigue Fract. Eng. Mater. Struct. 10 (1987) 93.
[5] C. Blochwitz, R. Richter, Mater. Sci. Eng. A267 (1999) 120.
[6] Groupe de Travail Matériaux EDF-CEA, T.43 RMA/GMM (77)3915 Document 9 (1978).
[7] M. Mineur, P. Villechaise, J. Mendez, Mater. Sci. Eng. 296 (2) (2000) 257.
[8] C. Laird, Y. Li, Mater. Sci. Eng. A 186 (1994) 87.
[9] C. Laird, Y. Li, Mater. Sci. Eng. A 186 (1994) 65.
[10] S. Heraud, Du polycristal au multicristal: élaboration d'un mésoscope numérique pour une analyse locale en élastoviscoplasticité, PhD Thesis, CEA R-5925120-129, 2000.
[11] C. Gorlier, Mécanismes de fatigue plastique de l'acier 316L sous formes monocristalline et polycrystalline. PhD Thesis, 2000.
[12] E. Ferrié, M. Sauzay, Mater. Sci. Forum. 567&568 (1999) 87.
[13] C. Blochwitz, W. Tirschler, A. Weidner, Mater. Sci. Eng. A 357 (1&2) (2003) 264.
[14] V. P Bennett, D.L. MacDowell, Eng. Fract. Mech. 70 (2003) 185.
[15] I. Simonovski, L. Cizel, Int. J. Fatigue 29 (9-1) (2007) 2005.
[16] S.R. Johnston, G.P. Potirniche, S.R. Daniewicz, M.F. Horstemeyer, Fatigue Fract. Eng. Mater. Struct. 29 (2006) 597.